Multi-objective optimization of gradient coil for benchtop magnetic resonance imaging system with high-resolution*

Wang Long-Qing(王龙庆) and Wang Wei-Min(王为民)†

Institute of Quantum Electronics, School of Electronic Engineering and Computer Science, Peking University, Beijing 100871, *China*

(Received 15 April 2013; revised manuscript received 3 May 2013; published online 10 December 2013)

Significant high magnetic gradient field strength is essential to obtaining high-resolution images in a benchtop magnetic resonance imaging (BT-MRI) system with permanent magnet. Extending minimum wire spacing and maximum wire width of gradient coils is one of the key solutions to minimize the maximum current density so as to reduce the local heating and generate higher magnetic field gradient strength. However, maximum current density is hard to optimize together with field linearity, stored magnetic energy, and power dissipation by the traditional target field method. In this paper, a new multi-objective method is proposed to optimize the maximum current density, field linearity, stored magnetic energy, and power dissipation in MRI gradient coils. The simulation and experimental results show that the minimum wire spacings are improved by 159% and 62% for the transverse and longitudinal gradient coil respectively. The maximum wire width increases from 0.5 mm to 1.5 mm. Maximum gradient field strengths of 157 mT/m and 405 mT/m for transverse and longitudinal coil are achieved, respectively. The experimental results in BT-MRI instrument demonstrate that the MRI images with in-plane resolution of 50 μm can be obtained by using the designed coils.

Keywords: magnetic resonance imaging, gradient coil, target field method, wire spacing

PACS: 87.61.–c, 84.32.Hh, 02.30.Zz **DOI:** 10.1088/1674-1056/23/2/028703

1. Introduction

Superconducting magnetic resonance imaging (MRI) is a powerful and mature noninvasive imaging method in biochemistry and clinical diagnosis. However, very high installation and running costs existing in superconducting MRI machines has restricted their availability for many research studies and they have also prevented the spread of this technology. The benchtop-MRI (BT-MRI) with permanent magnets can overcome this limitation due to much lower construction cost and almost zero running cost. In addition, it is more useful and convenient for some specific studies, such as small animal imaging, petroleum core analysis, drug delivery research, and micro-flow study, etc.[1–3] However, the existing BT-MRI equipment has relative low signal-to-noise ratio (SNR) due to the use of permanent magnet. Most of the materials to be analyzed have a longer T2 time in lower magnetic field than that in high magnetic field. Much higher SNR can be achieved if a very short echo time can be used for imaging. High gradient strength used for imaging slice selecting and frequency encoding in MR imaging can help a lot to shorten the echo time (TE) and increase SNR dramatically for high-resolution MR imaging. In order to obtain high-resolution imaging with echo time as short as 3 ms, field of view (FOV) = 25.6 mm×25.6 mm and an in-plane resolution of 50 μm, a read gradient strength of at least 150 mT/m is required which is far above the gradient strength (20 mT/m–30 mT/m) in medical MRI system. Therefore, designing gradient coils with very high gradient strength is essential for high resolution imaging in BT-MRI.

As important component of MRI, gradient coils are used to generate linear magnetic fields on the background of magnetic field for slice selection as well as phase and frequency encoding. The problem of designing a gradient coil is known as an inverse problem and can be described by a Fredholm equation of the first kind, which has a highly ill-posed nature.[4] Many theoretical methods have been developed for designing the gradient coils over the past several decades. One of the most famous methods is the target-field method, which was first proposed by Turner[5,6] in 1986 and has become the mainstream method of designing both shim coil and gradient coil in superconducting MRI. Turner's method can avoid the ill-posed nature of the problem using Fourier transform technique since the Fourier transform has unique inverses. The stream function technique[7,8] was used to discrete the current density into wires. A series of methods[9–12] based on the original have been developed. Forbes and Crozier[13–16] expressed the current density on the surface of coil by series expansion, and then use regularization technique to find the current density in the surface of the coil. Their method can be used to design the genuinely finite-length and asymmetric gradient coil. Morrone[17] used spherical harmonics to represent the target field and set high order coefficients to zero, which could achieve well coil performance in biplanar gradient coil design. Liu *et al.*[18] found that under certain physical and engineering conditions it is possible to obtain the desired

*Project supported by the Natural Science Foundation of the Ministry of Science and Technology of China (Grant No. 2011ZX05008004) and the Science Fund of the Committee of Science and Technology of Beijing, China.

†Corresponding author. E-mail: wmw@pku.edu.cn

© 2014 Chinese Physical Society and IOP Publishing Ltd

solutions by using a straightforward approach instead of using the Tikhonov regularization method. However, the maximum current density has never been optimized in past work, which must be considered in order to generate highest magnetic gradient field in BT-MRI instruments.

In this paper, a new design philosophy is used to design optimized maximum current density gradient coils. An objective function containing a maximum current density term is constructed. Besides, field accuracy, stored energy, and power dissipation are also optimized to achieve the best performances of coils. We have optimized all the above parameters via the accelerated gradient algorithm[19] due to the fact that this regularization problem has no analytic form. The design process and experimental results of transverse and longitudinal coil are presented.

2. Theory and method

2.1. Target field method

Figure 1 shows a sketch diagram of the geometry of coils and the target field locations. The direction of main magnetic field B_0 is aligned with z axis. The coils with current densities are located on the parallel plan ($z = \pm a$) and their radii (ρ) satisfy $\rho_{\min} < \rho < \rho_{\max}$. $P(x,y,z)$ represents a field point on the diameter of spherical volume (DSV) region in Cartesian coordinate while $S(\rho,\varphi)$ denotes a source point on the plane of gradient coil in polar coordinate. The components of the current density on the plane are expanded by a series of trigonometric basic functions as follows:

$$\begin{cases} J_\rho(\rho,\varphi) = \sum_{q=1}^{Q} U_q j_{\rho,q,k}(\rho)\sin k\varphi, \\ J_\varphi(\rho,\varphi) = \sum_{q=1}^{Q} U_q j_{\varphi,q,k}(\rho)\cos k\varphi, \end{cases} \tag{1}$$

where

$$\begin{cases} j_{\rho,q,k}(\rho) = \dfrac{k}{\rho}\{\chi_1 \sin[qc(\rho-\rho_{\min})] \\ \quad +\chi_2\{\cos[qc(\rho-\rho_{\min})] - 1 + q \bmod 2\}\}, \\ j_{\varphi,q,k}(\rho) = qc\{\chi_1 \cos[qc(\rho-\rho_{\min})] \\ \quad -\chi_2 \sin[qc(\rho-\rho_{\min})]\}, \end{cases} \tag{2}$$

in which $c = \pi/(\rho_{\max}-\rho_{\min})$, $\rho_{\min}$ is the minimum radius while $\rho_{\max}$ is the maximum, q and k are integers, χ_1 and χ_2 are 0 or 1 related to q and k in different forms for different designs. We set $\chi_1 = 1-(-1)^k$ and $\chi_2 = 1+(-1)^k$ in this paper. According to Eq. (1) it is known that in the areas of $\rho < \rho_{\min}$ and $\rho > \rho_{\max}$, $J_\rho = 0$, which means that the current is confined within a finite area. U_q is the coefficient of the q-th current density basic functions which are to be determined, Q is the order of the expansion. Q trends to infinity in theory; however, when Q is a finite number, such as 5 or 6, the finite order U_q can be accurate enough to determine the current density. The parameter k determines the order of the coils. In this paper, we set $k = 0$ and $k = 1$ for designing the longitudinal and transverse gradient coil, respectively. High order shimming coils can be designed by setting $k \geq 2$. It is noted that the expression of the current density satisfies the two-dimensional continuity equation

$$\nabla \cdot \boldsymbol{J} = \frac{1}{\rho}\left[\frac{\partial}{\partial\rho}(\rho J_\rho) + \frac{\partial J_\varphi}{\partial\varphi}\right] = 0. \tag{3}$$

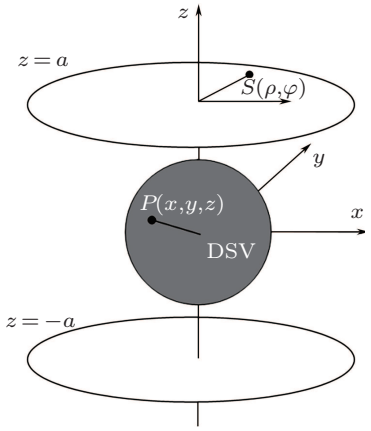


Fig. 1. Sketch diagram of the biplanar gradient coil system. A field point $S(\rho,\varphi)$ and a source point $P(x,y,z)$ are shown.

According to the Biot–Savart law, the magnetic field at field point, generated by the two current planes can be expressed as

$$\boldsymbol{B} = \frac{\mu_0}{4\pi}\int \frac{\boldsymbol{J}\times\boldsymbol{R}}{R^3}\,\mathrm{d}\sigma, \tag{4}$$

where μ_0 is the magnetic permeability of vacuum, $\boldsymbol{J}$ is the current density at the source point, $\boldsymbol{R}$ is the vector pointing from the source point to the field point, and $\mathrm{d}\sigma$ is the area element at the source point. In an MRI system, only the z component of magnetic field is considered, $B_z(x,y,z)$ generated by the current density on one plane of the biplanar coil can be obtained from the following equation:

$$B_z(x,y,z) = \frac{\mu_0}{4\pi}\int_{\rho_{\min}}^{\rho_{\max}}\int_0^{2\pi}\frac{\rho\,\mathrm{d}\rho\,\mathrm{d}\varphi}{R^3}D(\rho,\varphi), \tag{5}$$

where

$$\begin{aligned} D(\rho,\varphi) = {} & (J_\rho\cos\varphi - J_\varphi\sin\varphi)(y-\rho\sin\varphi) \\ & -(J_\rho\sin\varphi + J_\varphi\cos\varphi)(x-\rho\cos\varphi) \end{aligned} \tag{6}$$

with J_ρ and J_φ being, respectively, the radial and circumferential components of the current density in polar coordinates at source point on the coil plane in Eq. (1), and R is the distance from the source point to the point. Since the current densities on the two planes are identical for transverse coil while opposite for longitudinal coil, $B_z(x,y,z)$ generated by the two planar coils can be written as

$$B_z(x,y,z) = \frac{\mu_0}{4\pi}\int_{\rho_{\min}}^{\rho_{\max}}\int_0^{2\pi}\left(\frac{1}{R_+^3} \pm \frac{1}{R_-^3}\right)D(\rho,\varphi)\rho\,\mathrm{d}\rho\,\mathrm{d}\varphi, \tag{7}$$

where $R_{\pm} = \sqrt{(x-\rho\cos\varphi)^2+(y-\rho\cos\varphi)^2+(z\mp a)^2}$, R_+ denotes the distance between the space field point and the source point on the $z=+a$ plane while R_- represents the distance between the space field point and the source point on the $z=-a$ bottom plane. In Eq. (7), we use the plus sign '+' when the transverse gradient coil is designed, while the minus sign '–' is used to design longitudinal gradient coil.

Then, according to the current density in Eq. (1), B_z can be rewritten as

$$B_z(x,y,z) = \sum_{q=1}^{Q} U_q M_q(x,y,z), \tag{8}$$

where

$$\begin{aligned} & M_q(x,y,z) \\ &= \frac{\mu_0}{4\pi}\int_{\rho_{\min}}^{\rho_{\max}}\int_0^{2\pi}\left(\frac{1}{R_+^3}\pm\frac{1}{R_-^3}\right)(j_{\rho,q,k}(\rho)\sin k\varphi\cos\varphi \\ &\quad - j_{\varphi,q,k}(\rho)\cos k\varphi\sin\varphi)(y-\rho\sin\varphi) \\ &\quad - (j_{\rho,q,k}(\rho)\sin k\varphi\sin\varphi + j_{\varphi,q,k}(\rho)\cos k\varphi\cos\varphi) \\ &\quad \times (x-\rho\cos\varphi)\rho\,\mathrm{d}\rho\,\mathrm{d}\varphi. \end{aligned} \tag{9}$$

The element M_q is the function of the location of the space field point in the DSV and the integer q. If we set N target field points in DSV, equation (8) can be written as a matrix equation

$$B_z = MU, \tag{10}$$

where

$$B_z = \begin{bmatrix} B_{z1} \\ \vdots \\ B_{zN} \end{bmatrix}, \quad M = \begin{bmatrix} M_{11} & \cdots & M_{1Q} \\ \vdots & \ddots & \vdots \\ M_{N1} & \cdots & M_{NQ} \end{bmatrix}, \quad U = \begin{bmatrix} U_1 \\ \vdots \\ U_Q \end{bmatrix} \tag{11}$$

with B_z referring to a column vector of magnetic field values of all the N space field points $P(x,y,z)$. Each of all elements in M is a function of field point $P(x,y,z)$ and can be determined according to Eq. (9). The column vector U is the unknown coefficient of current density series in Eq. (1). In the traditional method, U is obtained by solving matrix equation (10). Using least squares method, U can be written as $U=(M^{\mathrm{T}}M)^{-1}(M^{\mathrm{T}}B)$, where M^{T} is the transpose of the matrix M. In this paper, we solve U by a multi-optimization method.

2.2. Optimization algorithm

In order to optimize wire spacing and achieve optimal performance of gradient coil, an objective function related to linearity, stored magnetic energy, power dissipation, and maximum current density is constructed in this section.

2.2.1. Linearity of gradient magnetic field

The linearity of the gradient magnetic field has a direct effect on the quality of MR image. The gradient coils with poor linearity will result in serious image distortion. This is the most important parameter that needs to be considered in all coil design methods in order to minimize the deviation of the field produced by the coil from the ideal gradient within the imaging region of interest (ROI). A field linearity objective function with respect to the total square errors of the z-axis component of the magnetic field at all target-field points can be written as $F_B = \sum_{n=1}^{N}(B_{z,n}-B_{z\mathrm{set},n})^2$, where $B_{z\mathrm{set},n}$ refers to the z component of the magnetic field which is set to obtain the desired gradient strength over a set of N target field points in the ROI and $B_{z,n}$, which is obtained by Biot–Savart law, is the actual field produced by the coil at the n-th point. Using Eq. (10) the field linearity objective F_B is written in a matrix form as

$$F_B = \sum_{n=1}^{N}(MU-B_{\mathrm{set}})^{\mathrm{T}}(MU-B_{\mathrm{set}}). \tag{12}$$

The linearity of $B_{z,n}$ can be evaluated by the local deviation of field from the desired value

$$\varepsilon = \max\left(\left|\frac{B_{z,n}-B_{z\mathrm{set},n}}{B_{z\mathrm{set},n}}\right|\right)\times 100\%. \tag{13}$$

Generally, linearity of the gradient magnetic field produced is required to not be higher than 5% in the ROI.

2.2.2. Stored magnetic energy

Optimization of the inductance which is related to stored magnetic energy must be considered in the design of gradient coil. Minimum inductance in the coil means a maximum slew rate, which is defined as the rate of change of gradient field per unit time, and high slew-rate can reduce imaging time and artifacts. The stored magnetic energy E of the gradient coils can be written as

$$E = \frac{1}{2}\int_V \boldsymbol{A}\cdot\boldsymbol{J}\,\mathrm{d}\upsilon, \tag{14}$$

where $\boldsymbol{A}$ is the magnetic vector potential produced by the current density vector $\boldsymbol{J}$ and V is the distributed volume of the current density. The stored magnetic energy can be further expressed as a quadratic form with respect to U [20]

$$E = \frac{1}{2}U^{\mathrm{T}}WU, \tag{15}$$

where W is an inductance fully symmetric and positive-definite matrix. The inductance L can be calculated by the equation

$$E = \frac{1}{2}LI^2, \tag{16}$$

where I represents the current in each turn conductor of coils.

2.2.3. Power dissipation

Minimizing power dissipation must also be considered in the design of a gradient coil. A low power dissipation in gradient coil can reduce the unwanted Joule heating of the gradient coil. The dissipated power P of the gradient coils in the system can be written as

$$P = \frac{\delta}{t}\iint_s |\boldsymbol{J}|^2 \mathrm{d}s, \tag{17}$$

where δ and t are the resistivity and thickness of the conducting material. Analogously, the power dissipation can be further expressed as a quadratic form with respect to U

$$P = \frac{1}{2}U^{\mathrm{T}}HU, \tag{18}$$

where H is a resistance matrix. H is also a symmetric and positive-definite matrix. The resistance can be evaluated by the equation

$$P = I^2R, \tag{19}$$

where I represents the current in each turn conductor of coils. It should be noted that the objectives of the inductance and resistance are conflicted with each other, low inductance results in high resistance sometimes, so a trade-off between them is needed in the design process.

2.2.4. Maximum current density

The maximum current density is optimized in order to reduce the local heat and improve the minimum wire spacing in the coil, so the coil is fabricated easily and can achieve the highest gradient magnetic field. The maximum current density magnitude in the coil design can be written as the l^{∞}-norm of the current density magnitude vector,[21] C is a matrix in which the maximum value represents the maximum current density at all surface points

$$\|J\|_{\infty} = \|J_C\|_{\infty} = \max_C\left(\sqrt{J_\rho^2 + J_\varphi^2}\right). \tag{20}$$

In order to solve U_q, an objective function is constructed as

$$F = \sum_{n=1}^{N}(B_{z,n} - B_{z\,\mathrm{set},n})^2 + \alpha E + \beta P + \gamma\|J\|_{\infty}, \tag{21}$$

where α, β, and γ are dimensionless weighting factors with respect to stored magnetic energy, power dissipation, and maximum current density respectively. The first term in Eq. (21) is the total square errors of z component magnetic field in ROI, which is related to the magnetic linearity. According to Eqs. (12), (15), and (18), the objective function can be rewritten in a matrix form as

$$F = \sum_{n=1}^{N}(D^{\mathrm{T}}U - B_{\mathrm{set}})(D^{\mathrm{T}}U - B_{\mathrm{set}})^{\mathrm{T}} + \frac{1}{2}\alpha U^{\mathrm{T}}WU + \frac{1}{2}\beta U^{\mathrm{T}}HU + \gamma\|J\|_{\infty}. \tag{22}$$

Since this multi-optimization problem has not an analytic solution, we minimize F using an accelerated gradient algorithm. It should be noted that the first term on the right-hand side in Eq. (22) must be within acceptable limits so that the linearity can be lower than 5%. The coil performance greatly depends on the choice of α, β, and γ, and we should balance their scaling so that low stored magnetic energy, low power dissipation, and large minimum wire spacing gradient coil can be achieved.

2.3. Stream function method

After the coefficients U_q are obtained, the winding patterns can be generated by the stream function method. Since the current density must satisfy the two-dimensional continuity equation, the introduced stream function satisfies the following equation:

$$\begin{cases} \dfrac{\partial S}{\partial \rho} = -J_\varphi, \\ \dfrac{\partial S}{\partial \varphi} = \rho J_\rho, \end{cases} \tag{23}$$

so S can be written as

$$S(\rho,\varphi) = -\sum_{q=1}^{Q} U_q\{\chi_1 \sin[qc(\rho-\rho_{\min})] + \chi_2\{\cos[qc(\rho-\rho_{\min})] - 1 + q \bmod 2\}\}\cos k\varphi.$$

Assuming that N_t turn winding lines are expected on the coil plane, we have

$$S = S_{\min} + (i-0.5)I, \quad i = 1,2,\ldots,N, \tag{24}$$

where

$$I_0 = \frac{S_{\max} - S_{\min}}{N_{\mathrm{t}}},$$

with $S_{\min}$ referring to the minimum value of the stream function while $S_{\max}$ represents the maximum value on the plane. The current in each winding line equals I_0.

3. Simulation results

The main magnet structure of BT-MRI system is illustrated in Fig. 2. The ROI is located in the center of the two planes with a diameter of 30 mm. Owing to the spatial symmetry, $N = 54$ target field points $P(id, jd, kd)$ in the first quadrant of ROI are considered to optimize the gradient coils, where i, j, and k must satisfy the inequality $(id)^2 + (jd)^2 + (kd)^2 \le r_0^2$ $i, j, k = 1,2,3,4$, where $d = r_0/4$, and r_0 is the radius of ROI, so a three-dimensional (3D) mesh in first quadrant is constructed. The magnetic fields of field points in other quadrants can be calculated by symmetry transform. In addition, the eddy currents will result in imaging interference, so a silicon steel plane is used in the system and the 2nd-order influence has been taken into account in the calculation model.

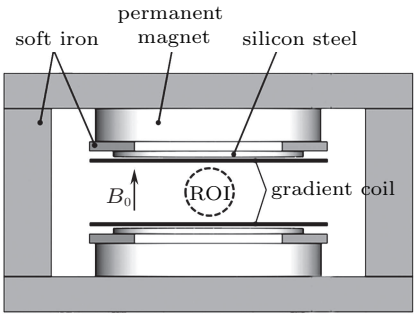


Fig. 2. Main magnet structure of the BT-MRI system.

The design parameters are different for the transverse and longitudinal gradient coil designs. In transverse gradient coil design, we set $k = 1$ in Eq. (1), $\rho_{\max} = 65$ mm, $\rho_{\min} = 0$ mm, and the number of coil turns $N_t = 20$. The z component magnetic field $B_{z\text{set},i}$ at all target field points are obtained by $B_{z\text{set},i} = G_x x_i$, $i = 1,2,\ldots,N$, where $G_x = 50$ mT·m^{-1}, x_i is the x coordinate of target field point. Analogously, in longitudinal gradient coil design, we set $k = 0$ in Eq. (1), $\rho_{\max} = 80$ mm, $\rho_{\min} = 0$ mm, and the number of coil turn $N_t = 16$. The z component magnetic field $B_{z\text{set},i}$ at all target field points are set by the equation $B_{z\text{set},i} = G_z z_i$, $i = 1,2,\ldots,N$, where $G_z = 50$ mT·m^{-1}, z_i is the z coordinate of target field point. Weighting factors for field linearity, stored magnetic energy, and power dissipation are $\alpha = 10^{-9}$, $\beta = 8 \times 10^{-17}$, and $\gamma = 4 \times 10^{-15}$ for transverse coil design, and $\alpha = 10^{-6}$, $\beta = 8 \times 10^{-11}$, and $\gamma = 4 \times 10^{-13}$ for longitudinal coil design. Comparative results of gradient coil design using two methods are shown in Table 1. Figure 3 shows the winding patterns of the gradient coil designed by the two methods.

From Table 1 it can be seen that for transverse gradient coil the inductance is reduced from 0.153 mH to 0.132 mH, the resistance is reduced from 0.952 Ω to 0.473 Ω, the coil efficiency is raised from 2.831 mT·m^{-1}·A^{-1} to 5.184 mT·m^{-1}·A^{-1} and the field linearity has almost no change. For longitudinal gradient coil, the inductance is reduced from 0.361 mH to 0.198 mH, the resistance is reduced from 0.898 Ω to 0.491 Ω, the coil efficiency is raised from 9.142 mT·m^{-1}·A^{-1} to 13.56 mT·m^{-1}·A^{-1} and the field linearity has almost no change. The current distribution compacted at some locations is hard to build and will generate high heating. Furthermore, the minimum wire spacing of transverse coil is raised from 0.680 mm to 1.761 mm, so maximum building wire width can be increased from 0.5 mm to 1.5 mm, while for longitudinal coil the minimum wire spacing is enhanced from 1.594 mm to 2.581 mm and maximum building wire width can be augmented from 1.3 mm to 2.3 mm, which can greatly increase the manufacturability of gradient coils and reduce local heating.

Figure 4(a) shows the magnetic field generated by the optimal transverse gradient coil at $y = 0$ plane in ROI. Figure 4(b) shows the magnetic field generated by the optimal transverse gradient coil at $z = 0$ plane between two coil surface. 20 μT·A^{-1} contour maps of the magnetic field and ROI are shown. The solid black line shows the region inside which the field linearity is less than 5%. The dash lines represent the coil surface. Similarly, figures 4(c) and 4(d) show the magnetic fields generated by the optimal longitudinal gradient coil.

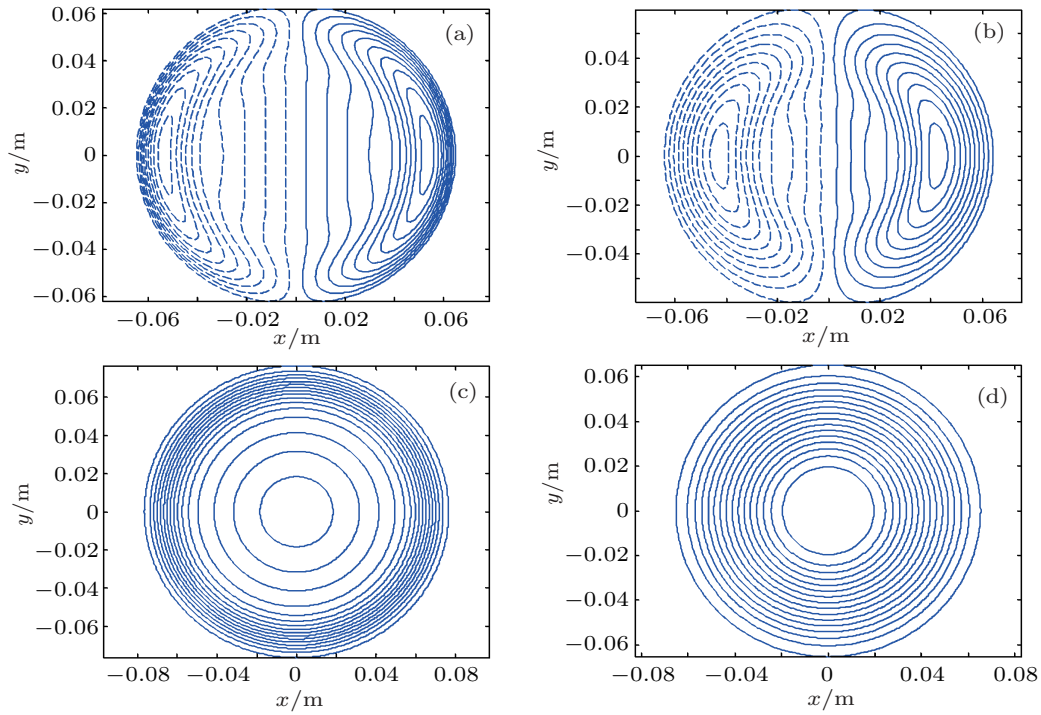


Fig. 3. (color online) Winding patterns for the transverse and longitudinal gradient coils using the traditional method ((a) and (c)) and the optimal method ((b) and (d)).

Table 1. Characteristics of gradient coil designed using optimal method and traditional method.

Property	Transverse gradient		Longitudinal gradient	
	Traditional method	Optimal method	Traditional method	Optimal method
Linearity/%	0.050	0.058	1.924	1.831
Efficiency/mT·m^{-1}·A^{-1}	2.831	5.184	9.142	13.56
Inductance/mH	0.153	0.132	0.361	0.198
Resistance/Ω	0.952	0.473	0.898	0.491
Minimum wire spacing/mm	0.680	1.761	1.594	2.581

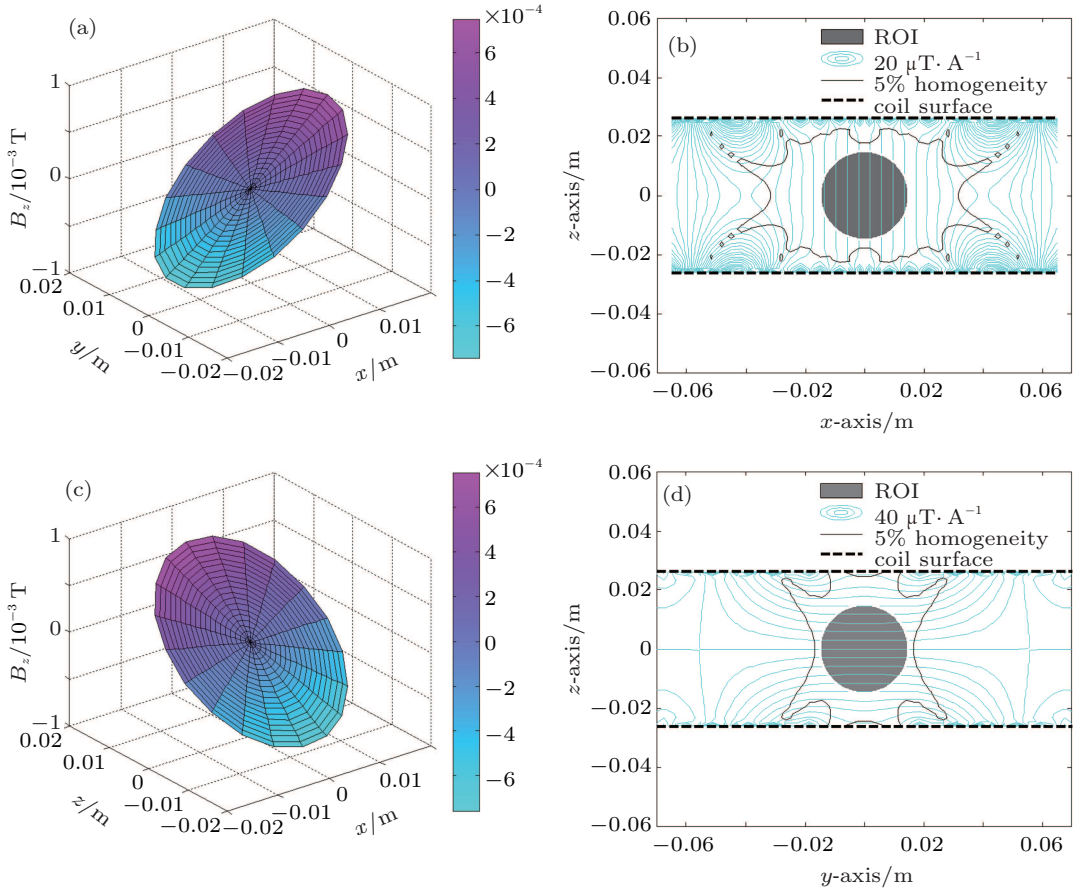


Fig. 4. (color online) Magnetic field distributions produced by the optimized transverse and longitudinal gradient coils.

4. Experiment results

To validate the calculation results, prototype coils are fabricated and tested in a home-made benchtop MRI system. The MRI system has a permanent magnet with a field strength of 0.46 T and an air gap of 58 mm. An RF coil with an inner diameter of 18 mm is used for both transmitting and receiving. A MARAN DRX console made by Oxford Instruments Inc. UK is adopted for MRI imaging acquisition and pulse sequence control.

A two-layer structure of wire is used for each coil of x, y, and z to avoid the direct return path of the wire that would affect the performance of coil. The gradient coil is made of printed circuit boards (PCB). The PCB copper trace used is 1.5 mm in width and 140 μm in thickness which has a current carrying capacity of 15 A. So the gradient strength can achieve 156 mT·m^{-1} and 405 mT·m^{-1} for transverse and longitudinal gradients, respectively. In total, six layers have been integrated in one PCB to manufacture the gradient coils for x, y, and z and result in a total thickness of 2 mm. Figure 5 shows the photographs of the prototype gradient coil set. The length of the gradient coils is 200 mm and their width is 200 mm.

A plastic phantom with a diameter of 15 mm is designed for MRI imaging testing in which different sizes of pore with diameters ranging from 0.3 mm to 2 mm (0.3, 0.8, 1.0, 1.2,1.5, 2.0 mm, respectively) have been drilled and shown in Fig. 6. The phantom is placed in a test tube filled with water, doped

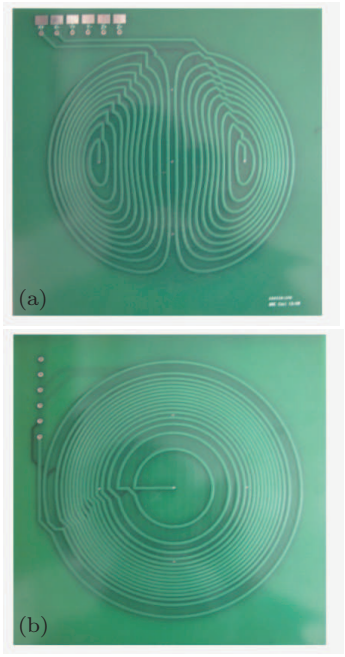


Fig. 5. (color online) Photographs of (a) transverse and (b) longitudinal prototype gradient coil set.

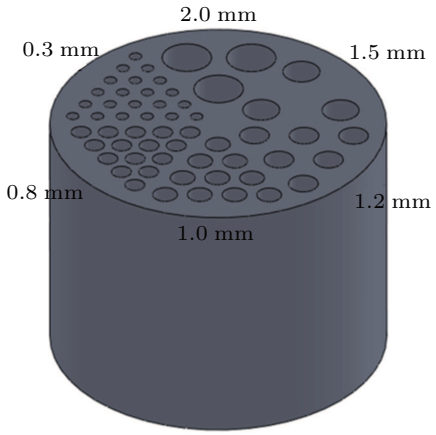


Fig. 6. (color online) Phantom designed for imaging.

with 0.5% $CuSO_4$ for imaging. Although gradient echo (GE) imaging sequence has a shorter imaging echo time, it is hard to use in BT-MRI for poor SNR. Figure 7 shows T1-weighted spin echo (SE) image of the phantom obtained with spin echo pulse sequence in the above MRI system. The experiment parameters are as follows: RF frequency (SF) = 19.58 MHz, repetition time (TR) = 150 ms, echo delay time (TE) = 3 ms, flip angle = 90°, the number of excitations (NEX) = 20, acquisition matrix size is 512×512, FOV = 25.6 mm×25.6 mm, and slice thickness = 0.7 mm. A very short spine echo time of 3 ms, which is about five times shorter than that used in medical MRI, has been achieved by using the new gradient coil. The maximum gradient used in the above imaging is 233 mT/m in the slice selection direction; that is, z direction. It can be seen that a group of pores each with a minimum diameter of 0.3 mm are clearly resolved and the in-plane resolution is better than 50 μm i.e., 25.6 mm/512 = 50 ìm which is about 20 times higher than that of the whole body medical MRI system using the SE imaging sequence. It proves that much high resolution MRI image can be achieved even in a low magnetic field BT-MRI system by using the designed gradient coils.

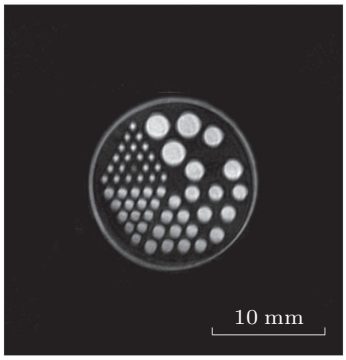


Fig. 7. T1-weighted image of phantom obtained with spin echo pulse sequence in 0.46-T BT-MRI system.

5. Conclusions

A new multi-objective approach to designing and optimizing the gradient coils with very high gradient strength for a benchtop MRI system with high-resolution is developed in this paper, which is based on the target field method and multi-objective optimization algorithm. The numerical and experimental results show that the minimum wire spacing and maximum wire width of the gradient coil are improved significantly under the condition of keeping the gradient coils with high linearity, low inductance, and small resistance. Applying the described method, a prototype of gradient coils for BT-MRI system is fabricated using the printed circuit board. The experimental results demonstrate that much higher resolution can be obtained in a low field permanent BT-MRI system. This method can also be applied in the designing and optimizing the active-shielded gradient and shim coils of an MRI system.

Acknowledgment

The author would like to thank Dr. Du Xiao-Ji for helpful discussion and comments on the manuscript.

References

[1] Choquet P, Breton E, Goetz C, Marin C and Constantinesco A 2009 *Phys. Med. Biol.* **54** 5287
[2] Malaterre V, Metz V, Ogorka J, Gurny R, Loggia N and Mäder K 2009 *J. Control. Release* **133** 31
[3] Metz H and Mäder K 2008 *Int. J. Pharm.* **364** 170
[4] Hidalgo-Tobon S S 2010 *Concepts Magn. Reson. A* **36** 223
[5] Turner R 1986 *J. Phys. D: Appl. Phys.* **19** 147
[6] Turner R 1988 *J. Phys. E: Sci. Instrum.* **21** 948
[7] Brideson M A, Forbes K L and Crozier S 2002 *Concepts Magn. Reson.* **14** 9

[8] Lemdisaov R A and Ludwig R A 2005 *Magn. Reson. B: Magn.Reson. Eng.* **26** 67
[9] Yoda K 1990 *J. Appl. Phys.* **67** 4349
[10] Carlson J W, Derby K A, Hawryszko K C and Weideman M 1992 *Magn. Reson. Med.* **26** 191
[11] Liu H and Truwit C L 1998 *IEEE Trans. Med. Imag.* **17** 826
[12] Liu W T, Zu D L and Tang X 2010 *Chin. Phys. B* **19** 018701
[13] Forbes L K and Crozier S 2001 *J. Phys. D: Appl. Phys.* **34** 3447
[14] Forbes L K and Crozier S 2002 *J. Phys. D: Appl. Phys.* **35** 839
[15] Forbes L K and Crozier S 2004 *IEEE Trans. Magn.* **40** 1929
[16] Forbes L K, Brideson M A and Crozier S 2005 *IEEE Trans. Magn.* **41** 2134
[17] Morreone T US Patent Number 5 760 582 1998
[18] Liu W T, Zu D L, Tang X and Guo H 2007 *J. Phys. D: Appl. Phys.* **40** 4418
[19] Hu C, Kwok J and Pan W 2009 *In NIPS* 781
[20] Zhang R, Xu J, Fu Y Y, Li Y J, Huang K F, Zhang J and Fang J 2011 *Meas. Sci. Technol.* **22** 125505
[21] Poole M, Weiss P, Lopez H S, Ng M and Crozier S 2010 *J. Phys. D: Appl. Phys.* **43** 095001